

Дистанционное зондирование сред

УДК 621.396

WEATHER APPLICATIONS OF DUAL-POLARIZATION RADARS

*Alexander Ryzhkov, Terry Schuur, Valery Melnikov,
Pengfei Zhang, Matthew Kumjian Dusan Zrnica*

Cooperative Institute for Mesoscale Meteorological Studies,
University of Oklahoma Norman, Oklahoma, USA.

E-mail: Alexander.Ryzhkov@noaa.gov.

Abstract—An overview of meteorological applications of polarimetric radars is presented. Both well proven implications of polarimetric radar measurements which are ready for operational implementation and promising new directions of research are outlined.

Introduction

World-scale modernization of existing weather radar networks by adding polarimetric capabilities is underway. Massive deployment of polarimetrically retrofitted NEXRAD radars in USA starts in 2011. Similar polarimetric upgrade has begun or about to start in several countries of Europe and Asia and Canada. The benefits of the dual-polarization radars for improvement of radar data quality, discrimination between different types of radar echo and hydrometeor species as well as for more accurate rainfall estimation has been successfully demonstrated in numerous research and validation studies [1 - 4].

A scheme with simultaneously transmitted and received waves of horizontal and vertical polarizations is selected for implementing on the operational radars [5]. According to this scheme, three polarimetric variables: differential reflectivity Z_{DR} , differential phase Φ_{DP} , and cross-correlation coefficient ρ_{hv} between orthogonally polarized radar returns are measured in addition to the reflectivity factor Z , mean Doppler velocity V , and Doppler spectrum width σ_v available from conventional single-polarization radars. An important polarimetric variable, specific differential phase K_{DP} is computed as a radial derivative of total differential phase Φ_{DP} .

A brief summary of major meteorological applications of polarimetric radars is presented herein.

Proven benefits of polarimetric weather radars

A. Improvement in data quality. Differential phase Φ_{DP} and its radial derivative K_{DP} are immune to radar miscalibration, attenuation caused by precipitation and wet radome, and partial beam blockage (PBB). Hence, these variables can be efficiently used for absolute calibration of radar reflectivity factor and its correction for attenuation and PBB using weather radar data. Polarimetric attenuation correction is especially important for the radars operating at shorter wavelengths. The concept of self-consistency of Z , Z_{DR} , and K_{DP} in rain is utilized for the data-based absolute calibration of radar reflectivity with the accuracy of 1 – 1.5 dB. Nonmeteorological radar echo (ground clutter, insects, birds, chaff, forest / grass fires) can be easily recognized and filtered out using polarimetric capability. Most of nonmeteorological targets (excluding man-made structures) are characterized by much lower cross-correlation coefficient ρ_{hv} than weather scatterers and simple thresholding of radar data based on ρ_{hv} effectively filters out nonweather echoes.

B. Classification. Polarimetric radars provide true multiparameter measurements which can be utilized for discrimination between different classes of hydrometeors. The operational algorithm for hydrometeor classification accepted for polarimetric NEXRAD distinguishes between light / moderate rain, heavy rain, rain dominated by big

drops (often associated with convective updrafts), mixture of rain and hail, dry snow, wet snow, graupel, and ice crystals. The hydrometeor classification algorithms (HCA) commonly utilize principles of fuzzy logic, decision-tree logic, and neural networks [6-7]. An example of the fields of Z , Z_{DR} , and ρ_{hv} measured in the mesoscale convective system (MCS) by the prototype of the polarimetric S-band WSR-88D radar and the corresponding results of radar echo classification are illustrated in Figs.1 and 2.

Biological scatterers and ground clutter are recognized ahead of a squall line. A leading edge of the squall line is marked by a thin line of “big drops” associated with size sorting caused by updrafts and wind shear followed by heavy rain and occasional hail. Gradual transition from rain to wet snow, dry snow, and crystals is observed in the stratiform part of MCS once the ray approaches melting level and overshoots it.

C. Rainfall estimation. Improvement in rainfall estimation is one of the greatest benefits of polarimetric radars. Such an improvement is a result of combined use of Z , Z_{DR} , and K_{DP} which helps to reduce the uncertainty caused by variability of drop size distributions inherent for conventional $R-Z$ relations. The improvement in radar data quality, identification and suppression of non-weather echoes, and utilization of the results of hydrometeor classification indirectly contribute to reducing the errors in radar rainfall estimates. The operational NEXRAD algorithm for polarimetric rainfall estimation is contingent on the output of HCA [8].

Figs.3 and 4 summarize the results of extensive validation study performed in Oklahoma using the micronet and mesonet rain gage networks [8]. In this study, 43 rain events and 179 hours of radar observations have been examined to quantify the biases and rms errors of hourly rainfall estimates as functions of the distance from the radar. Black curves correspond to the estimates from the conventional $R(Z)$ algorithm, whereas blue curves depict results obtained using the best polarimetric algorithm which utilizes Z , Z_{DR} , and K_{DP} as well as the results of hydrometeor classification.

The bias and rms errors of the hourly rain totals are reduced at the distances up to 200 km from the radar. The improvement is particularly significant at close distances where the rms error

is reduced roughly by a factor of 2. Combining hydrometeor classification and rainfall estimation helps to improve the accuracy of rain measurements at longer distances from the radar where the radar resolution volume is more likely to be filled with frozen or mixed-phase hydrometeors.

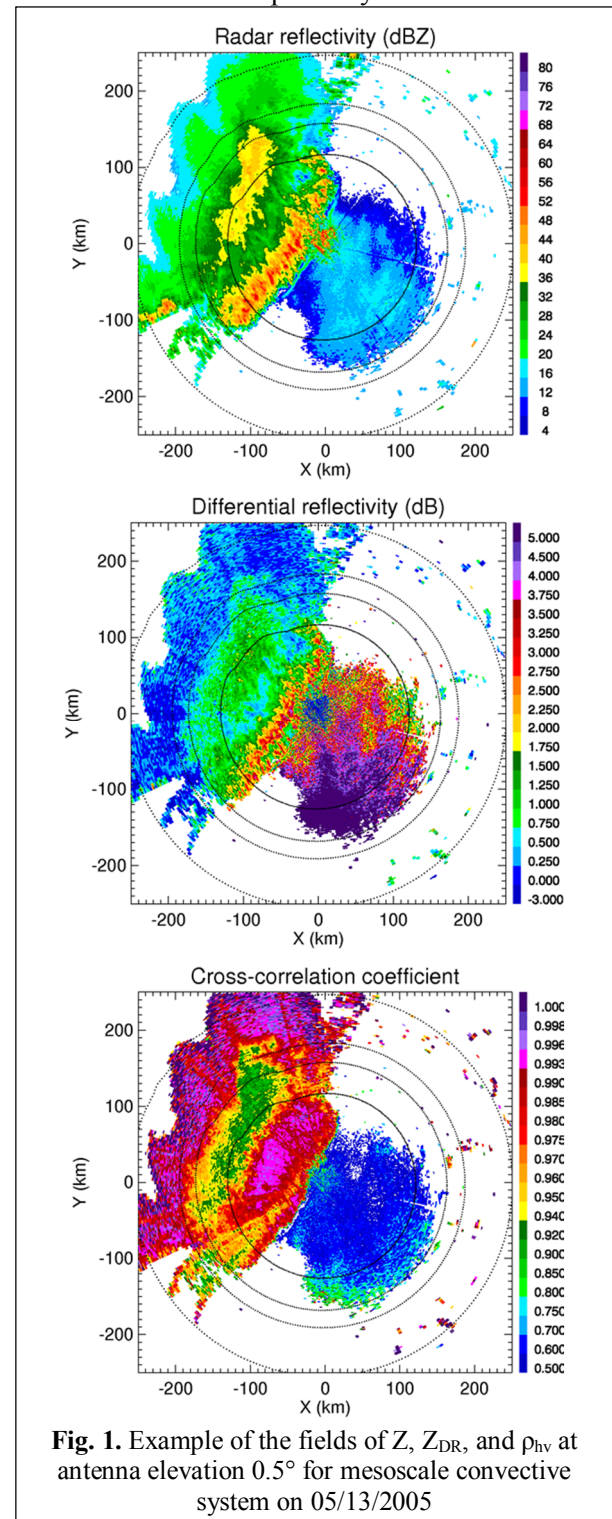


Fig. 1. Example of the fields of Z , Z_{DR} , and ρ_{hv} at antenna elevation 0.5° for mesoscale convective system on 05/13/2005

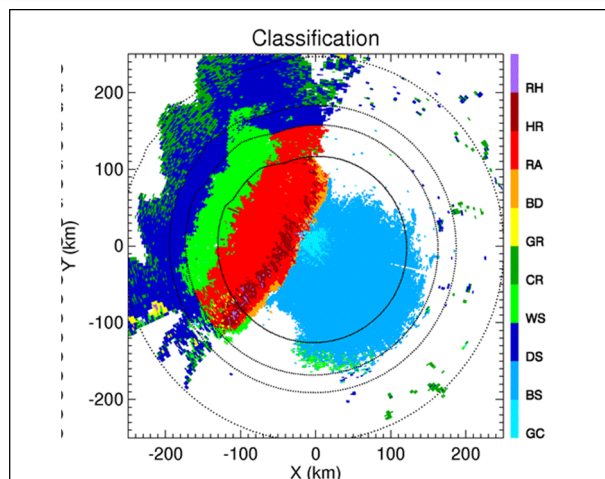


Fig. 2. Results of classification using the fields of polarimetric variables displayed in Fig. 1. GC – ground clutter/AP, BS – biological scatterers, DS – dry snow, WS – wet snow, CR – crystals, GR – graupel, BD – big drops, RA – rain, HR – heavy rain, RH – rain/hail

D. Tornado detection. Tornadoic debris produces discernible polarimetric signature which allows to reliably detect tornado on the ground [9]. In addition, vigorous size sorting in supercell storms leads to the pronounced increase of Z_{DR} at the southern flank of the storms. The corresponding signature, the “ Z_{DR} arc”, can be utilized for estimation of storm-relative helicity which can be utilized for tornado forecast [10 – 11].

The method for tornado detection with dual-polarization radar is illustrated in Fig. 5 where the fields of Z , Z_{DR} , and ρ_{hv} are displayed at the moment of tornado touchdown during the storm on 05/10/2003 in the Oklahoma City metropolitan area. A well-pronounced hook echo usually associated with potential development of tornado is clearly visible in the SW flank of the storm but identification of tornado on the ground can be reliably made only using the signatures in the Z_{DR} and ρ_{hv} fields. Dramatic drop in Z_{DR} and ρ_{hv} in the hook area signifies tornadoic debris up in the air.

It is important to document tornado occurrence. If the storm has a history of producing tornado, then it is likely that it may hit again. Using polarimetric radar is the only way to detect tornado in real time (not after the fact), especially in the dark or when tornado is wrapped in rain and is not visually observable.

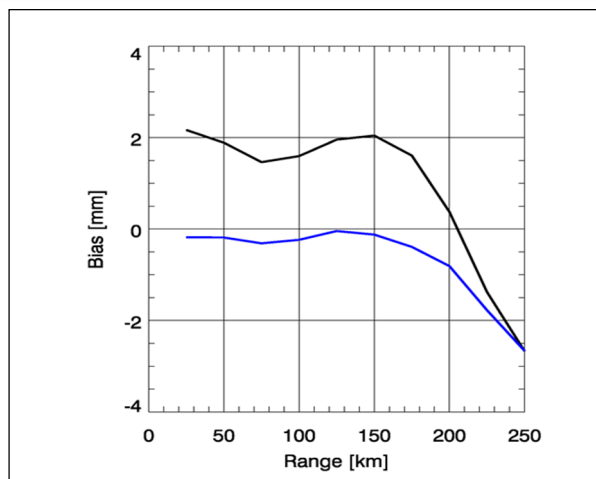


Fig. 3. The dependencies of the biases in hourly rain accumulation obtained from the conventional (black curve) and polarimetric (blue curve) estimators as functions of the distance from the radar. 43 events, 179 hours of observations

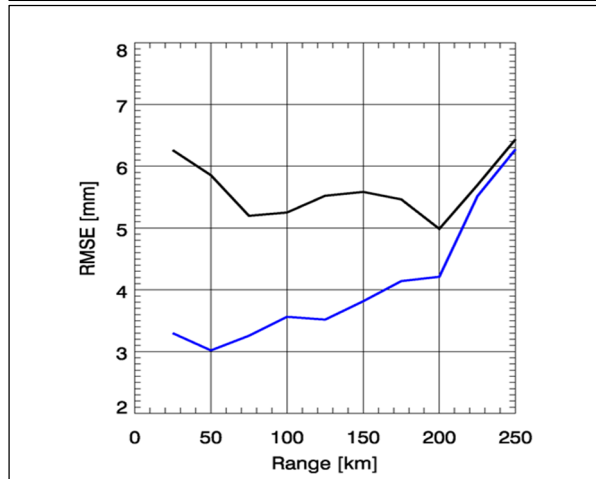


Fig. 4. Same as in Fig. 3 but for the rms error of hourly rain total estimate

E. Hail detection and determination of its size. As opposed to rain for which Z_{DR} increases with increasing Z , dry hail is usually characterized by high Z (which is not always the case) and low Z_{DR} caused by tumbling behavior of falling hailstones and low dielectric constant of ice.

However, once hailstones start melting, they acquire a coat of melted water which stabilizes their orientation and increases Z_{DR} . Most recent techniques for hail detection and determination of its size take into account this fact and make use of the height of the radar resolution volume with respect to the melting layer. There is strong evidence that discrimination between small hail ($D <$

2.5 cm), large hail (2.5 cm < D < 5.0 cm), and giant hail (D > 5.0 cm) is possible using polarimetric radar [12].

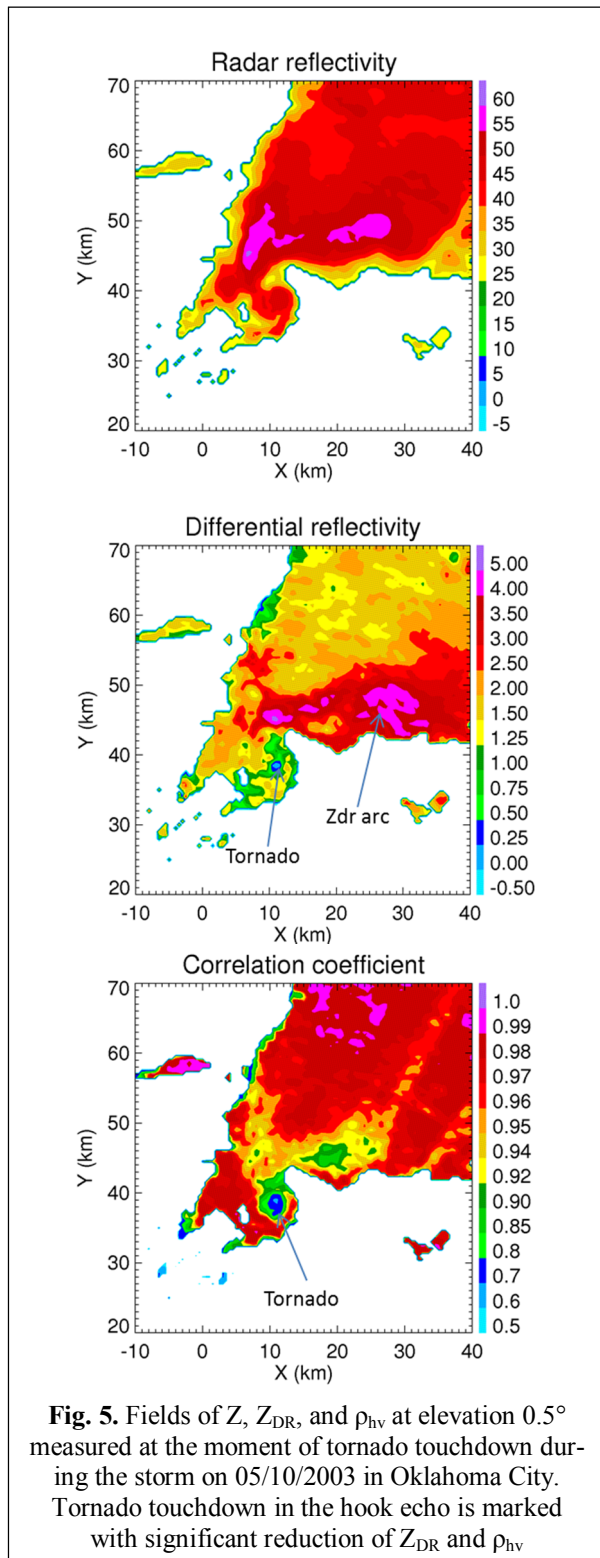


Fig. 5. Fields of Z , Z_{DR} , and ρ_{hv} at elevation 0.5° measured at the moment of tornado touchdown during the storm on 05/10/2003 in Oklahoma City. Tornado touchdown in the hook echo is marked with significant reduction of Z_{DR} and ρ_{hv}

It was shown in recent studies that giant hail is associated with noticeable depression of ρ_{hv} above

the melting level where hailstones are usually dry or have thin film of water on their surface if they grow in the “wet growth” regime. The corresponding Z_{DR} can be slightly negative due to the effects of resonance scattering although hail may have larger horizontal dimension. This means that in order to predict very large hail at the surface, one may look aloft in the storm where giant hail is formed.

The algorithm for hail detection initially developed at S band should be modified before applied at shorter wavelength, particularly at C band where large raindrops originated from melting hail may have anomalously high Z_{DR} which can overwhelm low intrinsic Z_{DR} of hail mixed with rain below the freezing level. Hence, melting hail mixed with rain usually has much higher Z_{DR} at C band compared to the measurements at S band.

F. Discrimination between rain and snow.

Ice particles with the same shape and orientation as raindrops have lower Z_{DR} and K_{DP} due to lower refractive index. These polarimetric parameters decrease with decreasing density of dry snow caused by aggregation. On the other hand, wet snow may be characterized by high Z_{DR} and low ρ_{hv} . Pristine ice crystals with very nonspherical shapes and the density of solid ice may produce high Z_{DR} and K_{DP} . These differences between polarimetric properties of rain and snow/ice of different types make possible a reliable discrimination not only between rain and snow in general but also between various habits of snow and ice.

An example of discrimination between rain, wet snow, and dry snow near the surface using C-band polarimetric radar is shown in Fig. 6. The RHI of radar reflectivity does not provide any clues about the type of precipitation near the surface. However, clear delineation between the three precipitation types can be reliably made using the Z_{DR} and especially the ρ_{hv} data. The melting layer descends to the surface west of the radar and the transition zone between pure rain and dry snow (i.e., wet snow) can be determined with remarkable precision.

New Promising applications

Additional polarimetric radar applications listed in this section are in their exploratory stage but there is enough observational evidence that they may offer significant benefits for meteorologists.

A. Convective initiation. It was shown in [13] that convective initiation and development may be monitored by examining “ Z_{DR} columns” indicating localization and strength of convective updrafts. These columns containing supercooled raindrops and graupel / hail undergoing dry or wet growth can stretch vertically well above the environmental freezing level depending on the strength of the updraft. The Z_{DR} columns can be utilized for prediction of subsequent development of heavy rain or hail as was shown in [13]. It turns out that the volume of the Z_{DR} column above the freezing level may characterize the intensity and type of the precipitation developed afterwards.

B. Freezing rain and icing. Freezing rain is one of the most dangerous phenomena associated with cold-season storms. If freezing rain is caused by melting of snowflakes within elevated warm layer, then it can be identified using polarimetric detection of the melting layer aloft. If the freezing rain is transformed into ice pellets within subfreezing surface layer, then such a transition is clearly seen by the increase of Z_{DR} because the process of re-freezing of supercooled liquid drops is accompanied by vigorous generation of nonspherical ice crystals. Utilizing polarimetric radar data together with thermodynamic information characterizing vertical profiles of temperature and humidity shows very good promise for detection of freezing rain and icing on the ground.

C. Quantification of snow. The benefits of polarimetric measurements for better quantification of snowfall have not been demonstrated yet. However, the ability of the dual-polarization radar to distinguish between snow of different density and to detect the formation of dendrites aloft as a major source of snow at the surface will eventually materialize in the improvement in snow measurements. More polarimetric radar observations accompanied with snow gage measurements in colder climates are needed to address this issue.

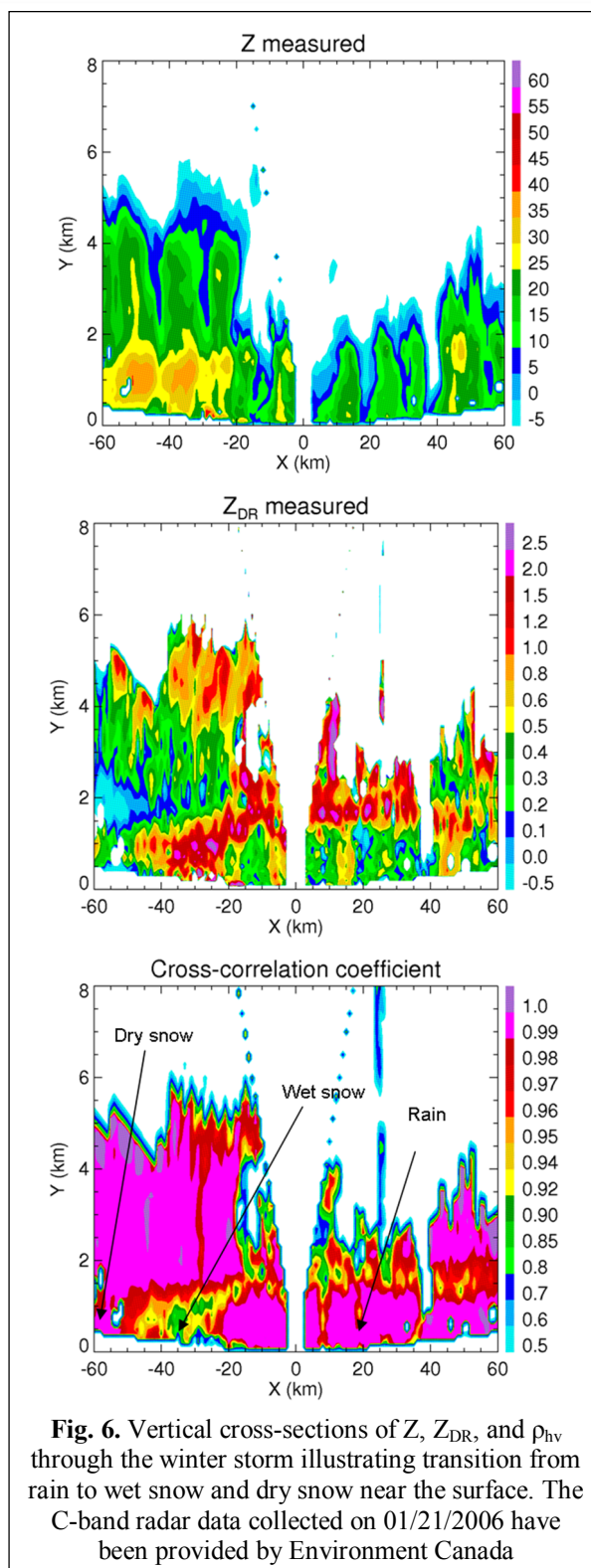


Fig. 6. Vertical cross-sections of Z , Z_{DR} , and ρ_{hv} through the winter storm illustrating transition from rain to wet snow and dry snow near the surface. The C-band radar data collected on 01/21/2006 have been provided by Environment Canada

D. Improvement in microphysical parametrization of NWP models. Inadequate microphysical parametrization (MP) of numerical weather prediction (NWP) models is one of the major factors restricting their capability for a more

accurate short-term storm forecast. Dual-polarization measurements coupled with cloud models offer unique chance to improve MP via better parametrization of size distributions of different hydrometeor species and via optimization of various parameters in equations characterizing rates of different microphysical processes. This is a new frontier of research which will potentially benefit NWP models and storm forecasting.

A series of theoretical and observational investigations of polarimetric signatures associated with different microphysical processes leading to the formation of precipitation (particle size sorting, evaporation, melting, refreezing) has been performed at the University of Oklahoma and National Severe Storms Laboratory in recent years. It was clearly shown that storm models with single-moment microphysical parametrization widely utilized for weather forecast can not adequately reproduce the observed polarimetric signatures in critical parts of the storm so that polarimetric radars are capable to provide crucial information for further modification of NWP models.

E. Assimilation of polarimetric radar data into NWP models. Another great opportunity is assimilation of polarimetric radar data into NWP models. The models, however, should be adequate to digest polarimetric data and successful assimilation is contingent on the improvement of MP in NWP. This is a big challenge for future studies.

References

1. Doviak, R.J. and D.S. Zrnice, 1993: Doppler radar and weather observations. Academic Press, 562 pp.
2. Bringi, V., and V. Chandrasekar 2001: Polarimetric Doppler Weather Radar. Principles and Applications. Cambridge University Press. 636 p.

3. Zrnice, D., and A. Ryzhkov, 1999 Polarimetry for weather surveillance radars. Bulletin of the American Meteorological Society, 80, 389 - 406.

4. Ryzhkov, A.V., T. J. Schuur, D.W. Burgess, S. Giangrande, and D.S. Zrnice, 2005: The Joint Polarization Experiment: Polarimetric rainfall measurements and hydrometeor classification. Bulletin of American Meteorological Society, 86, 809 – 824.

5. Doviak, R.J., V. Bringi, A.V. Ryzhkov, A. Zahrai, D.S. Zrnice, 2000: Considerations for polarimetric upgrades to operational WSR-88D radars. Journal of Atmospheric and Oceanic Technology, 17, 257 - 278.

6. Lim, S., V. Chandrasekar, and V.N. Bringi, 2005: Hydrometeor classification system using dual-polarization radar measurements: model improvements and in situ verification. IEEE Trans. Geosci. Rem. Sens., 43, 792 – 801.

7. Park, H.-S., A. Ryzhkov, D. Zrnice, and K.-E. Kim, 2009: The hydrometeor classification algorithm for the polarimetric WSR-88D. Description of application to an MCS. Weather and Forecasting, 24, 730 – 748.

8. Giangrande, S., and A. Ryzhkov, 2008: Estimation of rainfall based on the results of polarimetric echo classification. Journal of Applied Meteorology, 47, 2445 – 2462.

9. Ryzhkov A.V., T.J. Schuur, D.W. Burgess, and D.S. Zrnice, 2005: Polarimetric tornado detection. Journal of Applied Meteorology, 44, 557 – 570.

10. Kumjian, M. R., and A. Ryzhkov, 2008: Polarimetric signatures in supercell storms. Journal of Applied Meteorology and Climatology, 47, 1940 – 1961.

11. Kumjian, M., and 2009: Storm-relative helicity revealed from polarimetric radar measurements. Journal of Atmospheric Sciences, 66, 667 – 685.

12. Kumjian, M., J. Picca, S. Ganson, A. Ryzhkov, J. Krause, D. Zrnice, and A. Khain, 2010: Polarimetric characteristics of large hail. 25th Conference on Severe Local Storms. Denver, CO, Amer. Meteor. Soc., 11.2.

13. Picca, J., M. Kumjian, and A. Ryzhkov, 2010: Z_{DR} columns as a predictive tool for hail growth and storm evolution. 25th Conference on Severe Local Storms. Denver, CO, Amer. Meteor. Soc. 11.3.

Поступила 25 марта 2016 г.